Vibrationally Enhanced Hydrogen Tunneling in the *Escherichia coli* Thymidylate Synthase Catalyzed Reaction†

Nitish Agrawal, Baoyu Hong, Cornelia Mihai, and Amnon Kohen*

Department of Chemistry, University of Iowa, Iowa City, Iowa 52242

Received November 25, 2003; Revised Manuscript Received December 28, 2003

ABSTRACT: The enzyme thymidylate synthase (TS) catalyzes a complex reaction that involves forming and breaking at least six covalent bonds. The physical nature of the hydride transfer step in this complex reaction cascade has been studied by means of isotope effects and their temperature dependence. Competitive kinetic isotope effects (KIEs) on the second-order rate constant (*V/K*) were measured over a temperature range of 5−45 °C. The observed H/T ($^{T}V/K_{H}$) and D/T ($^{T}V/K_{D}$) KIEs were used to calculate the intrinsic KIEs throughout the temperature range. The Swain−Schaad relationships between the H/T and D/T *V/K* KIEs revealed that the hydride transfer step is the rate-determining step at the physiological temperature of *Escherichia coli* (20−30 °C) but is only partly rate-determining at elevated and reduced temperatures. H/D KIE on the first-order rate constant k_{cat} ($^{D}k = 3.72$) has been previously reported [Spencer et al. (1997) *Biochemistry 36,* 4212−4222]. Additionally, the Swain−Schaad relationships between that ^{D}k and the *V/K* KIEs reported here suggested that at 20 °C the hydride transfer step is the rate-determining step for both rate constants. Intrinsic KIEs were calculated here and were found to be virtually temperature independent ($\Delta E_a = 0$ within experimental error). The isotope effects on the preexponential Arrhenius factors for the intrinsic KIEs were $A_H/A_T = 6.8 \pm 2.8$ and $A_D/A_T = 1.9 \pm 0.25$. Both effects are significantly above the semiclassical (no-tunneling) predicted values and indicate a contribution of quantum mechanical tunneling to this hydride transfer reaction. Tunneling correction to transition state theory would predict that these isotope effects on activation parameters result from no energy of activation for all isotopes. Yet, initial velocity measurements over the same temperature range indicate cofactor inhibition and result in significant activation energy on k_{cat} (4.0 ± 0.1 kcal/mol). Taken together, the temperature-independent KIEs, the large isotope effects on the preexponential Arrhenius factors, and a significant energy of activation all suggest vibrationally enhanced hydride tunneling in the TS-catalyzed reaction.

Thymidylate synthase (TS)[1] (EC 2.1.1.45) catalyzes the last committed step in the de novo biosynthesis of 2′-deoxythymidine 5′-monophosphate (dTMP, one of the four building blocks of DNA). The enzyme catalyzes the reductive methylation of 2′-deoxyuridine 5′-monophosphate (dUMP) to dTMP. Apparently, two independent reactions are involved in which the cofactor N^5,N^{10}-methylene-5,6,7,8-tetrahydrofolate (CH_2H_4folate) serves as a donor of both methylene and hydride (*1*). The enzyme is crucial for DNA biosynthesis and is overexpressed in actively proliferating cells such as tumor cells (*2*). TS is the target of the widely used chemotherapeutic drug 5-fluorouracil (5-FU) which, after metabolism to 5-fluoro-2′-deoxyuridine 5′-monophosphate (5F-dUMP), acts as a potent inhibitor and is active against solid tumors such as those found in breast, head, neck, and colon cancers. However, to significantly inhibit large amounts of TS in tumor cells, high concentrations of TS inhibitory anticancer drugs are necessary. This harms normal tissue cells and results in toxicity. The use of TS inhibitors commonly lead to a further increase of TS expression levels in tumor cells (*3*), making it more difficult to achieve effective treatment without side effects and leading to drug resistance (*4*). A better understanding of the TS molecular mechanism may lead to more specific drugs that will specifically inhibit it in cancerous but not in normal cells. Additionally, preferable inhibition in bacterial but not in human cells can lead to antibiotic drugs.

TS from *Escherichia coli* (*ec*TS) has been extensively studied in terms of structure, kinetics, and mechanism (*1*, *5*, *6*). The enzyme is a homodimer with a molecular mass of 60 kDa. It is among the most highly conserved enzymes with approximately 18% of residues that are strictly conserved among at least 17 sequences (*7*). Numerous X-ray structures of free and bound enzyme−substrate−cofactor analogues have been determined, and several hundred mutants have been cloned and studied (*6*, *7*). Steady-state kinetic studies suggest a bi-bi order mechanism of reactants binding and products released (Scheme 1) (*1*).

† This work was supported by NIH Grant R01 GM65368-01 and NSF Grant CHE-0133117.

* Address correspondence to this author. Tel: 319-335-0234. E-mail: amnon-kohen@uiowa.edu.

[1] Abbreviations: TS, thymidylate synthase; DHFR, dihydrofolate reductase; KIE, kinetic isotope effect; RP HPLC, reverse-phase high-pressure liquid chromatography; LSC, liquid scintillation counter; 5-FU, 5-fluorouracil; 5-FdUMP, 5-fluoro-2′-deoxyuridine 5′-monophosphate; dUMP, 2′-deoxyuridine 5′-monophosphate; dTMP, 2′-deoxythymidine 5′-monophosphate; CH_2H_4folate, N^5,N^{10}-methylene-5,6,7,8-tetrahydrofolate; H_2folate, 7,8-dihydrofolate; H_4folate, 5,6,7,8-tetrahydrofolate; TEAA, triethylammonium acetate; QM H-tunneling, quantum mechanical hydrogen tunneling.

10.1021/bi036124g CCC: $27.50
Published on Web 01/29/2004

Scheme 1: Order of Substrate Binding and Product Release during the Catalytic Cycle of *E. coli* TS on the Basis of Initial Velocity and Product Inhibition Studies[a]

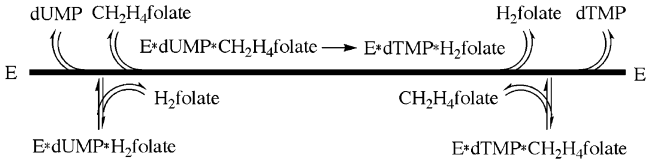

[a] Adapted from Carreras and Santi (*1*).

The overall reaction catalyzed by TS can be described as methyl for proton substitution at a vinylic carbon α to a carbonyl. A multistep reaction mechanism has been proposed in which TS transfers a methylene group from CH_2H_4folate to dUMP, followed by reduction of the methylene to methyl group to yield dTMP and H_2folate (Scheme 2). The formation of a ternary complex between enzyme, dUMP, and CH_2H_4folate aligns an overall conserved active site cysteine residue (Cys 146 in *E. coli*) that nucleophilically attacks the C-6 of dUMP (reaction 1 in Scheme 2). In *E. coli* TS, Glu 58 serves as a general base in the activation of the CH_2H_4-folate cofactor to form an iminium ion (A). Then, the C5 carbon of the activated enol (B) nucleophilically attacks the methylene Schiff base iminum ion (A) to form an enzyme-bound covalent intermediate (C) (*8*, *9*). This is followed by abstraction of a proton from C-5 dUMP (probably by Tyr 94 in *E. coli* as general base) to form the enol (D), which leads to the elimination of 5,6,7,8-tetrahydrofolate (H_4folate) to form the intermediate (E) (*10*). Finally, the exocyclic methylene intermediate is reduced by hydride from the 6*S* position of H_4folate to form dTMP and 7,8-dihydrofolate (H_2folate). It is not clear at this stage whether step 5 proceeds via another enolate intermediate or by an S_N2 fashion.

In this paper we present mechanistic studies of the hydride transfer step (reaction 5 in Scheme 2), in which tools of physical chemistry were developed to examine the possible contributions of quantum mechanical H-tunneling and enzyme/environmental motion to the TS-catalyzed reaction. Possible contributions of such phenomena to enzyme-catalyzed reactions are a matter of intensive research and have evoked substantial debate in recent years (*11*−*18*). In a recent review, Benkovic and Hammes-Schiffer (*19*) summarize the current state of "our understanding or ignorance" in the field of mechanistic enzymology. As emphasized in their discussion, the ability to expose and study the chemical step of interest within any enzymatic cascade is a major challenge and often the progress-limiting step. The work presented herein represents a study of one chemical step in such a complex chemical cascade. This work focuses on issues central to the discussion presented in ref *19*, namely, the contributions of tunneling and enzyme motion to the catalyzed reaction.

The nature of the hydride transfer step is examined by means of intrinsic KIEs, their temperature dependence, and activation parameters. The first temperature dependence of intrinsic KIEs has recently been reported by Francisco et al. (*20*), who studied peptidylglycine α-hydroxylating monooxygenase (PHM). Observed H/D and H/T KIEs were used to calculate intrinsic KIEs in a 5−45 °C temperature range. The method presented here for studying TS is different in several aspects from that used for PHM (*20*): (i) very different chemistry ($H^{\bullet}$ vs H^-), (ii) a unique labeling pattern, (iii) a new analytical methodology, and (iv) different data analysis. Yet, both studies reveal the degree and nature of quantum mechanical tunneling in an H-transfer catalyzed reaction.

Quantum mechanical tunneling is the phenomenon in which a particle transfers through a reaction barrier due to its wavelike properties (*21*−*23*). Quantum mechanical transfer of hydrogen at various oxidation states has been studied in several enzymatic systems. It was also associated with protein motion and its active site vibrations or other environmental fluctuations (*14*, *24*−*35*). This effect is often depicted as "dynamics", but here we will use the terminology of Benkovic, Hammes-Schiffer, Warshel, and others, in which dynamics are only nonequilibrium motions along the reaction coordinate (*12*, *19*, *36*, *37*). It is important to note that similar phenomena have also been reported for nonenzymatic systems as discussed below (*38*−*44*).

Kinetic complexity and commitment to catalysis were also investigated and analyzed in the context of previous studies

Scheme 2: Proposed Chemical Mechanism for the *E. coli* TS-Catalyzed Reaction[a]

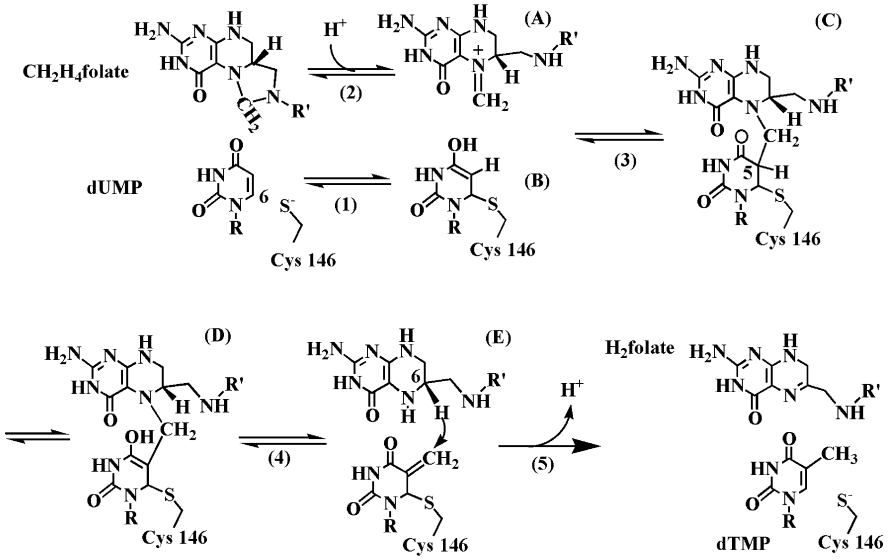

[a] Adapted from Carreras and Santi (*1*). R = 2′-deoxyribose 5′-phosphate and R′ = (*p*-aminobenzoyl)glutamate.

of noncompetitive KIEs at 20 °C (*5*). The research presented here involves a more complex pattern of isotopic labeling that enabled calculation of intrinsic KIEs. The current study also examines the temperature dependency, the cofactor inhibition, and the activation parameters of the rate constants and the intrinsic KIEs.

MATERIALS AND METHODS

Materials

Triethylammonium acetate (TEAA), acetonitrile (CH_3CN), dUMP, and dTMP were purchased from Sigma. CH_2H_4folate was a generous gift from Eprova Inc., Switzerland. The synthesis of the (*R*)-[6-^{3}H]CH_2H_4folate cofactor was described in detail elsewhere (*45*). In short, labeled $NaBH_4$ reduced acetone to labeled 2-propanol (*46*) that was then used to reduce $NADP^+$ to *R*-labeled NADPH with alcohol dehydrogenase from *Thermoanaerobium brockii* (*tb*ADH). This cofactor reduces H_2folate with DHFR to produce 6*S*-labeled H_4folate that yields (*R*)-[6-^{3}H]CH_2H_4folate upon quenching with formaldehyde. The specific radioactivity used in the kinetic experiments was 375 Ci/mol, which means that ~1% of the molecules were tritiated at the 6*R* position (the remainder was protonated at that position). A similar mixture of ~1% (*R*)-[6-^{3}H]CH_2H_4folate in (*R*)-[6-^{2}H]-CH_2H_4folate was synthesized by a similar procedure, but, instead, the synthesis was started from [^{3}H]$NaBH_4$ mixed with $NaBD_4$ (>99% D) to the same final specific activity. [2-^{14}C]dUMP (specific radioactivity 52 Ci/mol) was from Moravek Biochemicals. Tris(hydroxymethyl)aminomethane, ethylenediaminetetraacetic acid (EDTA), and β-mercaptoethanol were purchased from Sigma. Ultima Gold liquid scintillation cocktail and liquid scintillation vials were purchased from Packard Bioscience. The expression system for *E. coli* TS was a generous gift from R. Stroud (University of California at San Francisco). The enzyme was produced and purified at our laboratory following a published procedure (*47*). The HPLC system used was Agilent Technologies (previously HP) model 1100 equipped with an online degasser, quaternary pump, temperature-controlled column chamber, UV/Vis diode array detector, and manual injector. The column (C18, 250 × 4.6 mm, 5 μm, Discovery series) was from Supelco, and the column temperature was maintained at 25 °C. All analytical procedures are published in detail elsewhere (*45*).

Methods

Competitive Kinetic Isotope Effects. Primary H/T and D/T KIEs were measured competitively. All experiments were performed in 100 mM Tris buffer (pH = 7.5, adjusted at the experimental temperature), 50 mM β-mercaptoethanol, 1 mM EDTA, and 5 mM CH_2O. Prior to the kinetic experiments, the tritiated cofactor (trace (*R*)-[6-^{3}H]CH_2H_4folate in protiated or deuterated CH_2H_4folate for H/T or D/T KIE experiments, respectively) and ^{14}C-labeled substrate ([2-^{14}C]dUMP) were mixed (typically 1.5 Mdpm T with 0.5 Mdpm ^{14}C). To enable measurement of the fractional conversion of CH_2H_4folate to dTMP (*f*), the [2-^{14}C]dUMP was prepared in ~20% molar excess over the CH_2H_4folate as described in more detail elsewhere (*45*). The reaction mixture (final volume 1.1 mL) was preequilibrated at the experimental temperature. An aliquot of 100 μL was removed and quenched in 30 μM F-dUMP (a specific inhibitor of TS with K_i = 1 nM) and used to test the radiopurity of the reactants. The reaction was then initiated by addition of the enzyme, and five time points of 100 μL each were removed at 5 min intervals and quenched in 30 μM F-dUMP. Finally, a concentrated enzyme was added and incubated at the same temperature for an additional 10 min to achieve infinity time points. For each experiment, three infinity points were removed and quenched as described above. After quenching, all of the samples were frozen and stored at −80 °C prior to RP HPLC analysis. The ratio of ^{3}H/^{14}C in the product dTMP and the fractional conversion (*f*) were determined by RP HPLC separation, followed by fraction collection and liquid scintillation counter (LSC) analysis as described elsewhere (*45*). To calculate a KIE, three values were measured: the ratio of ^{3}H/^{14}C in the product at each time point (R_t), the ratio of ^{3}H/^{14}C at the infinity time points (R_∞), and the fractional conversion (*f*) (*23*):

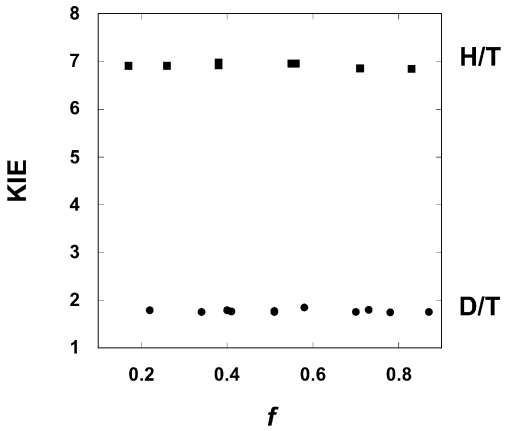

FIGURE 1: Competitive KIEs for primary $^TV/K_H$ (squares) and primary $^TV/K_D$ (circles) plotted vs fractional conversion (*f*) at 20 °C.

$$\mathrm{KIE} = \frac{\ln(1-f)}{\ln[1-f(R_t/R_\infty)]} \quad (1)$$

To determine *f*, the exact excess of [2-^{14}C]dUMP over CH_2H_4folate was measured from the infinity time points and was defined as % excess = [(total ^{14}C) − ([2-^{14}C]dTMP)$_\infty$]/(total ^{14}C).

f was then calculated from

$$f = \frac{[^{14}\mathrm{C}]\mathrm{dTMP}}{(100 - \%\ \mathrm{excess})([^{14}\mathrm{C}]\mathrm{dTMP} + [^{14}\mathrm{C}]\mathrm{dUMP})} \quad (2)$$

Figure 1 presents a typical plot of H/T and D/T KIEs vs fractional conversion. The fact that KIEs are *f* independent within experimental error serves as a good indication that no experimental artifact has affected the measurement (*23*, *48*). The value of the observed KIE at each temperature was the average of at least three independent experiments with five time points and three infinity points each.

Intrinsic KIEs. The intrinsic H/T KIEs were derived using the equation (*18*, *49*−*51*):

$$\frac{^T(V/K)^{-1}_{H,obs} - 1}{^T(V/K)^{-1}_{D,obs} - 1} = \frac{k_T/k_H - 1}{(k_T/k_H)^{1/3.34} - 1} \quad (3)$$

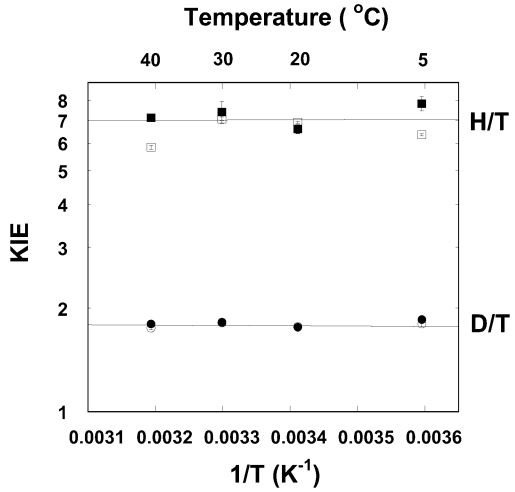

FIGURE 2: Arrhenius plot of observed (empty structures) and intrinsic (filled structures) primary $^{T}V/K_{H}$ (squares) and primary $^{T}V/K_{D}$ (circles). The intrinsic KIEs were calculated as discussed in the text. The lines are the exponential fitting of the intrinsic KIEs to eq 4 (*55*).

where $^{T}(V/K)_{H,obs}$ and $^{T}(V/K)_{D,obs}$ are the observed H/T and D/T KIEs, respectively. k_T/k_H is the reciprocal of k_H/k_T, which is the intrinsic H/T KIE. The intrinsic D/T KIE is formulated as $(k_H/k_T)^{1/3.34}$ (*18*, *52*). The Northrop procedure assumes that the reaction has no reverse commitment (or that EIE = 1) and that the Swain−Schaad relationship holds for intrinsic primary KIEs even if tunneling is involved (*18*, *51*). In this context, it is important to note that the TS reaction is indeed irreversible (no reverse commitment) and that, in systems demonstrated to proceed with tunneling, the experimental relationship between primary D/T and H/T KIEs is valued at, or very near, the semiclassical limit (*25*, *34*, *35*, *53*, *54*). Even if the magnitude of the exponent (3.34) was altered for a full tunneling model, it would not be expected to change within the temperature range of this study and, hence, would not affect any trend in intrinsic isotope effects with temperature (*20*). The only unknown in eq 3 is the intrinsic KIE (k_H/k_T). Since this equation cannot be solved analytically, a computer program was developed that solves it numerically. This program is now available on our web site http://cricket.chem.uiowa.edu/~kohen/ under tools.

The isotope effects on the activation parameters for the intrinsic KIEs were calculated by fitting them to the Arrhenius equation for isotope effects (*55*):

$$k_L/k_T = A_L/A_T e^{\Delta E_a/RT} \quad (4)$$

where L is H or D, A_L/A_T is the isotope effect on the preexponential Arrhenius factors, ΔE_a is the difference in energy of activation between T and L, *R* is the gas constant, and *T* is the absolute temperature (Figure 2).

Temperature and Concentration Dependence of Initial Rates. Initial velocities were measured by following the increase in absorbance at 340 nm which is due to the differences in absorbance between CH_2H_4folate and H_2folate [$\Delta\epsilon_{340nm}$= 6.4 $mM^{-1}cm^{-1}$ (*5*)]. Measurements were conducted with a Hewlett-Packard 8453 series UV/Vis spectrophotometer equipped with a temperature-controlled cuvette holder. Reaction mixtures containing various concentrations of substrate and cofactor in Tris buffer (pH = 7.5, adjusted at the experimental temperature), 50 mM DTT, 5 mM formaldehyde, and 1 mM EDTA were preincubated at the experimental temperature. The reaction was then initiated by addition of the enzyme. The absorbance at 340 nm (subtracted from the internal reference range of 420−450 nm) was measured in 2 s intervals. All measurements were done in at least triplicate, and data were analyzed as described below. These experiments were conducted with DTT instead of β-mercaptoethanol, since the latter is an inhibitor of the reaction (*10*).

Scheme 3: Labeling Patterns Used in the Competitive KIE Measurements[a]

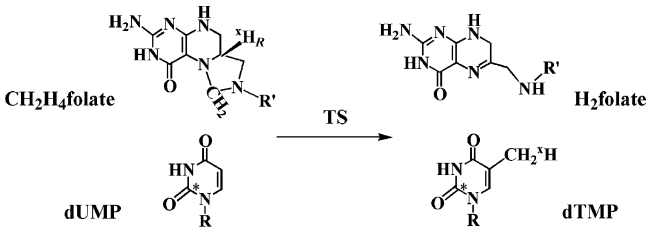

[a] An asterisk (*) represents a ^{14}C labeled at the C-2 position of dUMP, and ^{X}H represents an H, D, or T label at the 6*R* position of CH_2H_4folate. R = 2′-deoxyribose 5′-phosphate and R′ = (*p*-aminobenzoyl)glutamate.

RESULTS AND DISCUSSION

Competitive KIEs. Competitive *V/K* KIE measurements were conducted with 6*R* H-, D-, and T-labeled CH_2H_4folate and [2-^{14}C]dUMP. A unique feature of the competitive experiments presented here is that the remote ^{14}C label is not on the same reactant as the hydrogen isotope label (Scheme 3). Competitive KIE measurements of hydrogen isotopes are conducted by directly comparing the depletion or enrichment of the heavier isotope in product or reactant. For hydrogen isotopes, reactants with H or D are commonly labeled with ^{14}C or tritium at a remote position to enable measurement of their fractional conversion (*f*) (*18*, *29*, *56*). The procedure presented here involves a unique remote labeling of the H-acceptor (dUMP), while the donor is labeled with H, D, or T. The conversion of [2-^{14}C]dUMP to [2-^{14}C,7-^{X}H]dTMP is monitored, but the conversion of interest (*f*) is that of [6-^{X}H]CH_2H_4folate to [2-^{14}C,7-^{X}H]dTMP. This requires that the [2-^{14}C]dUMP be in excess (~20%) over CH_2H_4folate as described recently (*45*). ^{X}H represents H, D, or T, where X is 1, 2, or 3, respectively, and is transferred from the 6*R* position of CH_2H_4folate.

At 20 °C, competitive KIE experiments resulted in primary $_{T}V/K_{H}$ and $^{T}V/K_{D}$ KIEs of 6.91 ± 0.05 and 1.78 ± 0.02, respectively (Figure 1). The Swain−Schaad exponent for these KIEs is 3.35 ± 0.07, suggesting that the hydride transfer (step 5 in Scheme 2) is rate-determining overall (*18*, *51*). H/D KIE on k_{cat} (^{D}k = 3.72) has been measured at 20 °C by Spencer and co-workers (*5*) under the same experimental conditions as reported here. The Swain−Schaad exponent for the H/T *V/K* KIEs (reported here) vs the H/D k_{cat} KIEs (*5*) is 1.46 ± 0.4 [exp = $\ln(^{T}V/K_{H})/\ln(^{D}k)$]. Taken together, the exponential relationships of k_{cat} and *V/K* KIEs suggest no kinetic complexity on either k_{cat} or *V/K*, which strongly supports Spencer's suggestion that the hydride transfer step is rate-determining at 20 °C.

The reason that the observed primary KIEs are often smaller than the intrinsic ones is that kinetic steps that are

not isotopically sensitive "mask" the intrinsic KIEs as follows (*51*, *57*):

$$^{T}(V/K)_{L,obs} = \frac{k_L/k_T + C}{1 + C} \quad (5)$$

where C is the commitment to catalysis, which is the ratio between the rate of the isotopically sensitive step forward ($k_{H-transfer}$) and the rates of the preceding isotopically nonsensitive steps backward. Although no commitment is present at 20 and 30 °C, the commitment at 5 and 40 °C is 0.27 ± 0.05 (calculated from eq 5). This value suggests that the hydride transfer rate at these temperatures is not much slower than the rate of the reverse steps leading to the decomposition of complex E in Scheme 2 back to dUMP and CH_2H_4folate. Obviously, this fact cannot simply imply that the level of one forward step is "rate limiting" relative to other forward steps. In this paper we use the term "rate-determining step" for cases where the isotopically sensitive step is not masked by kinetic complexity (i.e., in a case of no commitment).

Temperature Dependence of Intrinsic KIEs. The measured H/T and D/T KIEs ($^{T}V/K_H$ and $^{T}V/K_D$, respectively) were used to calculate the intrinsic KIEs (k_H/k_T and k_D/k_T, respectively). The method developed by Northrop (*18*, *49*−*51*) was used to calculate the intrinsic KIE from the observed KIEs on the three isotopes of hydrogen (eq 3). Although this equation has only one unknown (k_H/k_T), it cannot be solved analytically, and a program that offers numerical solutions to any form of the Swain−Schaad relationship is now available to the public on our web site as listed above. Statistical analysis of the error propagation is not trivial since eq 3 cannot be derivatized for k_H/k_T. The error propagation we chose was to avoid averaging the observed KIE. Instead, the intrinsic KIEs were calculated for all combinations of the observed H/T and D/T KIEs from individual measurements under the same conditions. This solution is similar to the one applied by Francisco et al. (*20*) and would underestimate the 95% confidence interval (due to the large number of combinations). Nevertheless, this procedure leads to a realistic standard deviation. The average intrinsic KIE and its standard deviation were used in calculating the isotope effects on the activation parameters (Figure 2).

Figure 2 presents an Arrhenius plot (KIE on a logarithmic scale vs the reciprocal of the absolute temperature) for the observed and intrinsic H/T and D/T KIEs. Two features are apparent from this figure: (i) The intrinsic KIEs are temperature independent over the temperature range examined and within experimental errors. (ii) The observed KIEs are close to the intrinsic values at the enzyme's physiological temperature (20−30 °C), but the observed KIEs are smaller at elevated and reduced temperatures. The first point was examined by exponential fit of the KIEs to eq 4 (*55*). The isotope effects on E_a (ΔE_a) were indeed close to zero (0.02 ± 0.25 and −0.04 ± 0.08 kcal/mol for H/T and D/T KIEs, respectively). The isotope effects on the Arrhenius preexponential factors were $A_H/A_T = 6.77 \pm 2.78$ and A_D/A_T 1.90 ± 0.27. Both of these values lie well above the semiclassical limit (1.67 and 1.22 for H/T and D/T, respectively) and cannot be explained by a tunneling correction for the light particle (*22*, *23*, *41*, *58*, *59*). The values are, however, characteristic of a reaction in which both the light and heavy isotopes tunnel. A number of examples of this behavior in both enzymatic reactions (*27*, *35*, *60*) and nonenzymatic reactions (*38*−*44*) now exist in the literature. Yet only one previous study has reported intrinsic KIEs that are free from complication of kinetic complexity (*20*).

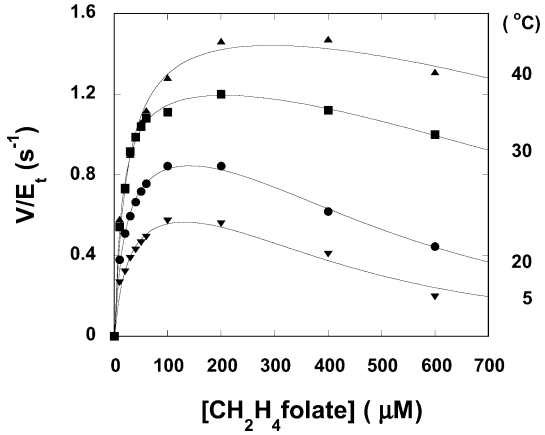

FIGURE 3: Steady-state initial velocity rates vs CH_2H_4folate concentration at 0.1 mM dUMP. The lines are the nonlinear root mean square fit to eq 6 (*55*, *62*).

Temperature Dependence of Initial Rates. The steady-state initial velocities were measured within a temperature range of 5−40 °C. At each temperature, CH_2H_4folate concentrations were varied from 10 to 600 μM with a fixed dUMP concentration of 100 μM. Alternatively, dUMP concentrations were varied from 25 to 600 μM at 150 μM CH_2H_4folate. The observed initial velocities were divided by the enzyme concentration prior to data analysis. The rates measured with dUMP as the variable substrate followed the Michaelis−Menten hyperbolic equation (*61*), while those measured with varying CH_2H_4folate concentrations presented substrate inhibition (Figure 3) and were fitted to the equation (*62*):

$$v = k_{cat}[S]/(K_M + [S](1 + [S]^2/K_S)) \quad (6)$$

where [S] is the varying substrate concentration, k_{cat} is the first-order rate constant, K_M is the Michaelis constant, and K_S is the substrate inhibition constant. Figure 3 shows the rate (v) vs CH_2H_4folate concentration in 100 μM dUMP. The lines represent the nonlinear fit of the data to eq 6 (*55*). This pattern of inhibition is in accordance with the bi-bi ordered mechanism in which dUMP binds prior to CH_2H_4folate, and H_2folate release precedes that of dTMP (Scheme 1) (*1*). In a previous report, Spencer and co-workers (*5*) suggested that the binding constant for CH_2H_4folate might be larger than 100 μM at 20 °C. Fitting of the data presented here (Figure 3) at 20 °C to eq 6 results in $K_S = 280 \pm 24$ mM, which is indeed a relatively large inhibition constant. Yet, inclusion of the cofactor inhibition while calculating k_{cat} is of substantial importance, since fitting of the observed rates to the Michaelis equation without cofactor inhibition leads to an underestimation of k_{cat}. This is especially important in the examination of the energy of activation on k_{cat}, because K_S's temperature dependence is very significant (22 ± 2 kcal/mol). If not accounted for, this affects the observed temperature dependence of k_{cat}. The first-order rate constant k_{cat} at each temperature was obtained from eq 6, and the data were fit to the Arrhenius equation (Figure 4) (*55*). The energy of activation on k_{cat} (E_a) was determined to be 4 ± 0.1 kcal/

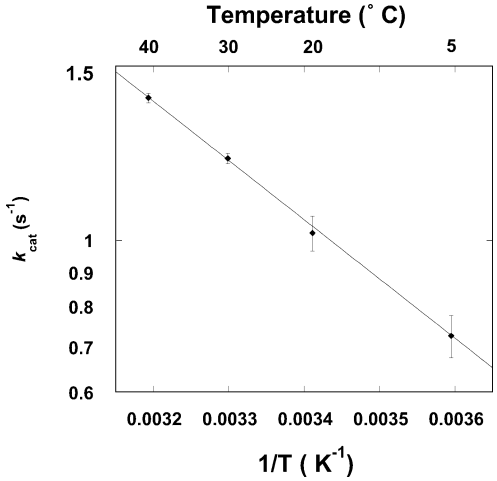

FIGURE 4: Arrhenius plot of k_{cat} (logarithmic scale) calculated from fitting the data presented in Figure 3 to eq 6. The line is the exponential fitting of the data to the Arrhenius equation (*55*).

mol ($\Delta H^{\ddagger}_{25°C} = 3.4 \pm 0.08$ kcal/mol and $S^{\ddagger} = 24 \pm 12$ kcal mol^{-1} deg^{-1}). Interestingly, activation energy close to 4 kcal/mol is relatively small, and typical hydride transfer has enthalpy of activation closer to 8−15 kcal/mol (*13*). Nevertheless, this E_a is too large to fit theories that suggest no thermal activation as a source of temperature-independent KIEs (*14*). The significance of this finding on the mechanism of hydride transfer in the TS-catalyzed reaction is discussed below.

Environmentally Enhanced Tunneling. The data presented above enable close examination of the nature of the hydride transfer step (step 5, Scheme 2) in the complex catalytic cascade of the *ec*TS reaction. The temperature-independent KIEs with large A_L/A_T taken together with $E_a = 4$ kcal/mol are not in accordance with theoretical models that use tunneling correction where both the light and heavy isotopes tunnel (*14*, *35*). This is because such models explain the lack of temperature dependence of KIEs by assuming no temperature dependence on the reaction rates for both light and heavy isotopes [full, or extensive, tunneling model (*13*, *16*, *18*)]. The fact that E_a is significantly larger than zero might be explained by models that invoke an isotopically insensitive, thermally activated, step (e.g., environmental pre- or rearrangement) and an isotopically sensitive but temperature-independent H-transfer step (tunneling) (*14*, *16*, *19*, *27*). Temperature-independent KIEs with a large energy of activation have been reported in the literature (*20*, *30*, *32*, *33*, *35*, *63*, *64*). Those findings also could not be understood by applying a simple correction to transition state theory, and a "Marcus-like" model that included an environmental motion was applied. An environmental motion can alter the probability of achieving configurations with degenerate quantum states. Such a motion can also alter the probability of tunneling at the degenerate configurations (*15*, *16*, *27*, *60*, *65*−*68*). These types of environmental motion modulate the tunneling barrier, typically by modulating the driving force of the reaction, the reorganization energy [$E°$ and λ in Marcus theory (*69*, *70*)], and the degeneracy of the reactant and product energy levels. Several terms have been coined in models that describe such phenomenon, including "vibrationally enhanced ground-state quantum tunneling" (*60*), "rate-promoting vibrations" (*66*), and "environmentally coupled tunneling" (*16*, *27*). All of these models are phenomenological, and no molecular level calculations have yet been reported that can reproduce such phenomenon.

An alternative way to analyze the contributions of tunneling, coupled motion, dynamics, and other physical phenomena to an enzymatic reaction rate would be to simulate the reaction using hybrid quantum mechanics/molecular mechanics (QM/MM) calculations. Such calculations were performed for several other enzymatic H-transfer reactions (e.g., refs *36*, *37*, *68*, and *71*−*75*). Those simulations were commonly done for systems where results from KIE and other studies suggested nonclassical contributions to those enzymatic reactions. Despite the medical importance of this enzyme and its interesting chemical reaction, no such calculations have been conducted for TS. This might be due to the lack of experimental information relevant to intrinsic processes along the reaction coordinate. Maybe the data presented here will encourage such studies.

Contributions to Catalysis. It is of great interest to assess the contribution of nonclassical phenomenon to enzyme catalysis. To address that issue, the catalyzed and uncatalyzed reactions must be compared. Early attempts to address this question were carried out by Kreevoy, Cleland, Schowen, and their co-workers (*76*−*78*). Unfortunately, it is not commonly possible to measure the rate or KIE of uncatalyzed reactions that are relevant to an enzyme-catalyzed reaction. Most uncatalyzed or nonenzymatically catalyzed reactions lead to many byproducts and may proceed through a transition state other than the enzymatic one. Wolfenden and co-workers (*79*) demonstrated a rare exception for the hydrolytic reaction, and recently Finke and co-workers (*80*, *81*) studied a model system with potential relevance to the methylmalonyl-CoA mutase reaction (*82*). In this last study, moderate tunneling (tunneling of only the light particle) was suggested for a model reaction from $A_H/A_D < 1$. That result is very different from the results presented here (A_H/A_T and $A_D/A_T > 1$) but is qualitatively similar to that reported for the methylmalonyl-CoA mutase catalyzed reaction (*82*). In their papers, Finke and co-workers suggested that their results are in accordance with a similar degree of tunneling in both enzymatic and nonenzymatic systems. In our minds, since the H-transfer is not rate-determining in that enzymatic reaction and since the uncatalyzed reaction was initiated by photolysis (potentially leading to a vibrationally excited state for the H-transfer), it is not yet clear how general that suggestion might be.

CONCLUSIONS

The hydride transfer step in the wild-type *ec*TS-catalyzed reaction was examined, and several significant conclusions can be drawn from the findings reported above. This work provides the first experimental evidence for a contribution of vibrationally enhanced quantum mechanical tunneling to the hydride step in a TS-catalyzed reaction. The temperature independence of the primary KIEs is key evidence of nonclassical behavior. The temperature dependence of intrinsic primary KIEs yields isotope effects on Arrhenius parameters that lie well outside the semiclassical limits (*22*, *23*, *58*, *59*).

Cofactor inhibition of CH_2H_4folate was observed while measuring the steady-state rate constants across the temper-

ature range (5−40 °C). This phenomenon was predicted by previous publications for the reaction at 20 °C (*1*, *5*) but was never observed before. This finding is in accordance with the kinetic mechanism presented in Scheme 1. The inhibition constant has a large binding energy (22 kcal/mol) such that inhibition almost vanishes at elevated temperature. Accounting for this inhibition enabled extraction of the first-order rate constant k_{cat} at all temperatures and afforded calculation of its energy of activation ($E_a = 4 \pm 0.1$ kcal/mol). This, together with the KIE activation parameters, suggests that the *ec*TS-catalyzed H-transfer involves environmentally enhanced (vibrationally coupled) tunneling.

At the current state of "our understanding or ignorance" (*19*), no one specific model that has been developed to explain temperature-independent KIEs seems to be more general than others. Thus, we use the term "environmentally enhanced tunneling" (*16*, *27*) while addressing "Marcus-like" models. This term seems to be more comprehensive because it includes both preorganizational motion (affecting the symmetry of the H-transfer coordinate) and the "gating" fluctuation (primarily affecting the barrier's width). We hope that the new findings presented here will enable and encourage theoreticians to embark on a molecular investigation (e.g., QM/MM studies) of this interesting system.

Whether phenomena such as H-tunneling, vibrationally coupled tunneling, and environmentally enhanced reaction rates contribute to enzyme catalysis is an open question. Further studies of enzymatically relevant model reactions using the tool described here could lead to a more concrete evaluation of that seminal question.

ACKNOWLEDGMENT

The authors are grateful to Dr. Maley from Wadsworth Institute, State Department of Health, Albany, NY, for an initial supply of the purified enzyme and for fruitful discussions. The authors thank Dr. Rudolf Moser, Eprova, Switzerland, for the generous gift of standard CH_2H_4folate. The authors also thank Mr. Scott Tharp for assistance. Finally, we thank Drs. Daniel Quinn, Richard Schowen, and Judith Klinman for reading the original manuscript and for useful suggestions.

REFERENCES

1. Carreras, C. W., and Santi, D. V. (1995) The catalytic mechanism and structure of thymidylate synthase, *Annu. Rev. Biochem. 64*, 721−762.
2. von Laar, J. A., Rustum, Y. M., Ackland, S. P., van Groeningen, C. J., and Peters, G. J. (1998) Comparison of 5-fluoro-2′-deoxyuridine with 5-fluorouracil and their role in the treatment of colorectal cancer, *Eur. J. Cancer 34*, 296−306.
3. Salonga, D., Danenberg, K. D., Johnson, M., Metzger, R., Groshen, S., Tsao-Wei, D. D., Lenz, H. J., Leichman, C. G., Leichman, L., Diasio, R. B., and Danenberg, P. V. (2000) Colorectal tumors responding to 5-fluorouracil have low gene expression levels of dihydropyrimidine dehydrogenase, thymidylate synthase, and thymidine phosphorylase, *Clin. Cancer Res.*, 1322−1327.
4. Copur, S., Aiba, K., Drake, J. C., Allegra, C. J., and Chu, E. (1995) Thymidylate synthase gene amplification in human colon cancer cell lines resistant to 5-fluorouracil, *Biochem. Pharmacol. 49*, 1419−1426.
5. Spencer, H. T., Villafranca, J. E., and Appleman, J. R. (1997) Kinetic scheme for thymidylate synthase from *Escherichia coli*: determination from measurements of ligand binding, primary and secondary isotope effects, and pre-steady-state catalysis, *Biochemistry 36*, 4212−4222.
6. Finer-Moore, J. S., Santi, D. V., and Stroud, R. M. (2003) Lessons and conclusions from dissecting the mechanism of a bisubstrate enzyme: thymidylate synthase mutagenesis, function and structure, *Biochemistry 42*, 248−256.
7. Stroud, R. M., and Finer-Moore, J. S. (2003) Conformational dynamics along an enzymatic reaction pathway: Thymidylate Synthase,"the Movie", *Biochemistry 42*, 239−247.
8. Moore, M. A., Ahmed, F., and Dunlap, R. B. (1986) Trapping and partial characterization of an adduct postulated to be the covalent catalytic ternary complex of thymidylate synthase, *Biochemistry 25*, 3311−3317.
9. Hyatt, D. C., Maley, F., and Montfort, W. R. (1997) Use of strain in a stereospecific catalytic mechanism: crystal structures of *Escherichia coli* thymidylate synthase bound to FdUMP and methylenetetrahydrofolate, *Biochemistry 36*, 4585−4594.
10. Barrett, J. E., Maltby, D. A., Santi, D. V., and Schultz, P. G. (1998) Trapping of the C5 methylene intermediate in thymidylate synthase, *J. Am. Chem. Soc. 120*, 449−450.
11. Warshel, A., Jen, C. Y., and Villa, J. (2001) Do dynamically driven tunneling effects contribute in a major way to enzyme catalysis?, *Biophys. J. 80*, 144−151.
12. Warshel, A., and Parson, W. W. (2001) Dynamics of biochemical and biophysical reactions: insight from computer simulations, *Q. Rev. Biophys. 34*, 563−679.
13. Kohen, A., and Klinman, J. P. (1998) Enzyme catalysis: beyond classical paradigms, *Acc. Chem. Res. 31*, 397−404.
14. Kohen, A., and Klinman, J. P. (1999) Hydrogen tunneling in biology, *Chem. Biol. 6*, R191−R198.
15. Antoniou, D., and Schwartz, S. D. (2001) Internal enzyme motions as a source of catalytic activity: rate-promoting vibrations and hydrogen tunneling, *J. Phys. Chem. B 105*, 5553−5558.
16. Knapp, M. J., and Klinman, J. P. (2002) Environmentally coupled hydrogen tunneling. Linking catalysis to dynamics, *Eur. J. Biochem. 269*, 3113−3121.
17. Klinman, J. P. (2003) Dynamic barriers and tunneling. New views of hydrogen transfer in enzyme reactions, *Pure Appl. Chem. 75*, 601−608.
18. Kohen, A. (2003) Kinetic isotope effects as probes for hydrogen tunneling, coupled motion and dynamics contributions to enzyme catalysis, *Prog. React. Kinet. Mech. 28*, 119−156.
19. Benkovic, S. J., and Hammes-Schiffer, S. (2003) A perspective on enzyme catalysis, *Science 301*, 1196−1202.
20. Francisco, W. A., Knapp, M. J., Blackburn, N. J., and Klinman, J. P. (2002) Hydrogen tunneling in peptidylglycine-hydroxylating monooxygenase, *J. Am. Chem. Soc. 124*, 8194−8195.
21. Atkins, P., and De-Paula, J. (2002) *Physical Chemistry*, 7th ed., Oxford University Press, Oxford.
22. Bell, R. P. (1980) *The tunnel effect in chemistry*, Chapman and Hall, London and New York.
23. Melander, L., and Saunders, W. H. (1987) *Reaction rates of isotopic molecules*, Krieger Publishing Co., Malabar, FL.
24. Cha, Y., Murray, C. J., and Klinman, J. P. (1989) Hydrogen tunneling in enzyme reactions, *Science 243*, 1325−1330.
25. Grant, K. L., and Klinman, J. P. (1989) Evidence that both protium and deuterium undergo significant tunneling in the reaction catalyzed by bovine serum amine oxidase, *Biochemistry 28*, 6597−6605.
26. Glickman, M. H., Wiseman, J. S., and Klinman, J. P. (1994) Extremely large isotope effects in the soybean lipoxygenase-linoleic acid reaction, *J. Am. Chem. Soc. 116*, 793−794.
27. Knapp, M. J., Rickert, K., and Klinman, J. P. (2002) Temperature-dependent isotope effects in soybean lipoxygenase-1: Correlating hydrogen tunneling with protein dynamics, *J. Am. Chem. Soc. 124*, 3865−3874.
28. Bahnson, B. J., Park, D. H., Kim, K., Plapp, B. V., and Klinman, J. P. (1993) Unmasking of hydrogen tunneling in the horse liver alcohol dehydrogenase reaction by site-directed mutagenesis, *Biochemistry 32*, 5503−5507.
29. Bahnson, B. J., and Klinman, J. P. (1995) Hydrogen tunneling in enzyme catalysis, in *Enzyme Kinetics and Mechanism*, pp 373−397, Academic Press, San Diego.
30. Basran, J., Sutcliffe, M. J., Hille, R., and Scrutton, N. S. (1999) Reductive half-reaction of the H172Q mutant of trimethylamine dehydrogenase: evidence against a carbanion mechanism and assignment of kinetically influential ionizations in the enzyme−substrate complex, *Biochem. J. 341*, 307−314.

31. Basran, J., Sutcliffe, M. J., and Scrutton, N. S. (1999) Enzymatic H-transfer requires vibration-driven extreme tunneling, *Biochemistry 38*, 3218−3222.
32. Harris, R. J., Meskys, R., Sutcliffe, M. J., and Scrutton, N. S. (2000) Kinetic studies of the mechanism of carbon−hydrogen bond breakage by the heterotetrameric sarcosine oxidase of *Arthrobacter* sp. 1-IN, *Biochemistry 39*, 1189−1198.
33. Basran, J., Sutcliffe, M. J., and Scrutton, N. S. (2001) Deuterium isotope effects during carbon−hydrogen cleavage by trimethylamine dehydrogenase, *J. Biol. Chem. 276*, 24581−24587.
34. Jonsson, T., Edmondson, D. E., and Klinman, J. P. (1994) Hydrogen tunneling in the flavoenzyme monoamine oxidase B, *Biochemistry 33*, 14871−14878.
35. Kohen, A., Cannio, R., Bartolucci, S., and Klinman, J. P. (1999) Enzyme dynamics and hydrogen tunneling in a thermophilic alcohol dehydrogenase, *Nature 399*, 496−499.
36. Hwang, J. K., Chu, Z. T., Yadav, A., and Warshel, A. (1991) Simulations of quantum mechanical corrections for rate constants of hydride-transfer reactions in enzymes and solutions, *J. Phys. Chem. 95*, 8445−8448.
37. Villa, J., and Warshel, A. (2001) Energetics and dynamics of enzymatic reactions, *J. Phys. Chem. B 105*, 7887−7907.
38. Kwart, H. (1982) Temperature dependence of primary kinetic isotope effect as a mechanistic criterion, *Acc. Chem. Res. 15*, 401−408.
39. Anhede, B., and Bergman, N. A. (1984) Transition-state structure and the temperature dependence of the kinetic isotope effect, *J. Am. Chem. Soc. 106*, 7634−7636.
40. Braun, J., Schwesinger, R., Williams, P. G., Morimoto, H., Wemmer, D. E., and Limbach, H. H. (1996) Kinetic H/D/T isotope and solid-state effects on the tautomerism of the conjugate porphyrin monoanion, *J. Am. Chem. Soc. 118*, 11101−11110.
41. Brunton, G., Griller, D., Barclay, L. R. C., and Ingold, K. U. (1976) Kinetic applications of electron paramagnetic resonance spectroscopy. 26. Quantum-mechanical tunneling in the isomerization of sterically hindered aryl radicals, *J. Am. Chem. Soc. 98*, 6803−6811.
42. Koch, H. F., Dahlberg, D. B., McEntee, M. F., and Klecha, C. J. (1976) Use of kinetic isotope effects in mechanism studies. Anomalous Arrhenius parameters in the study of elimination reactions, *J. Am. Chem. Soc. 98*, 1060−1061.
43. Kresge, A. J., and Powell, M. F. (1981) Absence of internal return in the reaction of (4-nitrophenyl)nitromethane with amine bases in toluene solution. Implication on unusually large isotope effects reported for this reaction, *J. Am. Chem. Soc. 103*, 201−202.
44. Butenhoff, T. J., and Moore, C. B. (1988) Hydrogen atom tunneling in the thermal tautomerism of porphine imbedded in a *n*-hexane matrix, *J. Am. Chem. Soc. 110*, 8336−8341.
45. Agrawal, N., Mihai, C., and Kohen, A. (2003) Microscale Synthesis of isotopically labeled *R*-[6-^{x}H]-N5,N10-methylene 5,6,7,8-tetrahydrofolate as a substrate for thymidylate synthase, *Anal. Biochem.* (in press).
46. Agrawal, N., and Kohen, A. (2003) Microscale synthesis of 2-tritiated isopropanol and 4R-tritiated reduced nicotinamide adenine dinucleotide phosphate, *Anal. Biochem. 322*, 179−184.
47. Changchien, L.-M., Garibian, A., Frasca, V., Lobo, A., Maley, G. F., and Maley, F. (2000) High-level expression of *Escherichia coli* and *Bacillus subtilis* thymidylate synthase, *Protein Expression Purif. 19*, 265−270.
48. Rucker, J., Cha, Y., Jonsson, T., Grant, K. L., and Klinman, J. P. (1992) Role of internal thermodynamics in determining hydrogen tunneling in enzyme-catalyzed hydrogen transfer reactions, *Biochemistry 31*, 11489−11499.
49. Northrop, D. B. (1975) Steady-state analysis of kinetic isotope effects in enzymatic reactions, *Biochemistry 14*, 2644−2651.
50. Northrop, D. B. (1977) Determining the absolute magnitude of hydrogen isotope effects in *Isotope effects on enzyme-catalyzed reactions* (Cleland, W. W., O'Leary, M. H., and Northrop, D. B., Eds.) pp 122−152, University Park Press, Baltimore, MD.
51. Northrop, D. B. (1991) Intrinsic isotope effects in enzyme catalyzed reactions in *Enzyme mechanism from isotope effects* (Cook, P. F., Ed.) pp 181−202, CRC Press, Boca Raton, FL.
52. Streitwieser, A., Jagow, R. H., Fahey, R. C., and Suzuki, F. (1958) Kinetic isotope effects in the acetolyses of deuterated cyclopentyl tosylates, *J. Am. Chem. Soc. 80*, 2326−2332.
53. Bahnson, B. J., Colby, T. D., Chin, J. K., Goldstein, B. M., and Klinman, J. P. (1997) A link between protein structure and enzyme catalyzed hydrogen tunneling, *Proc. Natl. Acad. Sci. U.S.A. 94*, 12797−12802.
54. Chin, J. K., and Klinman, J. P. (2000) Probes of a role for remote binding interactions on hydrogen tunneling in the horse liver alcohol dehydrogenase reaction, *Biochemistry 39*, 1278−1284.
55. Curve fitting: Curve fitting was carried out as a least root-mean-square, standard deviations weighted, nonlinear regression with the software Kaleidagraph.
56. Cook, P. F. (1991) *Enzyme mechanism from isotope effects*, CRC Press, Boca Raton, FL.
57. Cleland, W. W. (1991) Multiple isotope effects in enzyme-catalyzed reactions, in *Enzyme Mechanism from Isotope Effects* (Cook, P. F., Ed.) pp 247−268, CRC Press, Boca Raton, FL.
58. Stern, M. J., and Weston, R. E., Jr. (1974) Phenomenological manifestations of quantum-mechanical tunneling. III. Effect on relative tritium−deuterium kinetic isotope effects, *J. Chem. Phys. 60*, 2815−2821.
59. Schneider, M. E., and Stern M. J. (1972) Arrhenius preexponential factors for primary hydrogen kinetic isotope effects, *J. Am. Chem. Soc 94*, 1517−1522.
60. Sutcliffe, M. J., and Scrutton, N. S. (2002) A new conceptual framework for enzyme catalysis. Hydrogen tunneling coupled to enzyme dynamics in flavoprotein and quinoprotein enzymes, *Eur. J. Biochem. 269*, 3096−3102.
61. Fersht, A. (1998) *Structure and mechanism in protein sciences: a guide to enzyme catalysis and protein folding*, W. H. Freeman, New York.
62. Charlier, J., H. A., and Plapp, B. V. (2000) Kinetic cooperativity of human liver alcohol dehydrogenase, *J. Biol. Chem. 275*, 11569−11575.
63. Basran, J., Patel, S., Sutcliffe, M. J., and Scrutton, N. S. (2001) Importance of barrier shape in enzyme-catalyzed reactions—vibrationally assisted tunneling in tryptophan tryptophylquinone-dependent amine dehydrogenase, *J. Biol. Chem. 276*, 6234−6242.
64. Maglia, G., and Allemann, R. K. (2003) Evidence for environmentally coupled hydrogen tunneling dihydrofolate reductase catalysis, *J. Am. Chem. Soc. 125*, 13372−13373.
65. Borgis, D., and Hynes, J. T. (1993) Dynamical theory of proton tunneling transfer rates in solution—general formulation, *Chem. Phys. 170*, 315−346.
66. Antoniou, D., Caratzoulas, S., Kalyanaraman, C., Mincer, J. S., and Schwartz, S. D. (2002) Barrier passage and protein dynamics in enzymatically catalyzed reactions, *Eur. J. Biochem. 269*, 3103−3112.
67. Bruno, W. J., and Bialek, W. (1992) Vibrationally enhanced tunneling as a mechanism for enzymatic hydrogen transfer, *Biophys. J. 63*, 689−699.
68. Agarwal, P. K., Billeter, S. R., and Hammes-Schiffer, S. (2002) Nuclear quantum effects and enzyme dynamics in dihydrofolate reductase catalysis, *J. Phys. Chem. B 106*, 3283−3293.
69. Marcus, R. A. (1982) Electron, proton and related transfers, *Faraday Discuss. Chem. Soc. 74*, 7−15.
70. Marcus, R. A., and Sutin, N. (1985) Electron transfer in chemistry and biology, *Biochim. Biophys. Acta 811*, 265−322.
71. Agarwal, P. K., Webb, S. P., and Hammes-Schiffer, S. (2000) Computational studies of the mechanism for proton and hydride transfer in liver alcohol dehydrogenase, *J. Am. Chem. Soc. 122*, 4803−4812.
72. Alhambra, C., Sánchez, M. L., Corchado, J. C., Gao, J., and Truhlar, D. J. (2001) Quantum mechanical tunneling in methylamine dehydrogenase, *Chem. Phys. Lett. 347*, 512−518.
73. Alhambra, C., Corchado, J. C., Sánchez, M. L., Gao, J., and Truhlar, D. J. (2000) Quantum dynamics of hydride transfer in enzyme catalysis, *J. Am. Chem. Soc. 122*, 8197−8203.
74. Cui, Q., Elstner, M., and Karplus, M. (2002) A theoretical analysis of the proton and hydride transfer in liver alcohol dehydrogenase (LADH), *J. Phys. Chem. B 106*, 2721−2740.
75. Cui, Q., and Karplus, M. (2001) Triosephosphate isomerase: A theoretical comparison of alternative pathways, *J. Am. Chem. Soc. 123*, 2284−2290.
76. Ostovic, D., Roberts, R. M. G., and Kreevoy, M. M. (1983) Isotope effects on hydride transfer between NAD^+ analogues, *J. Am. Chem. Soc. 105*, 7629−7631.
77. Hermes, J. D., and Cleland, W. W. (1984) Evidence from multiple isotope effect determinations for coupled hydrogen motion and tunneling in the reaction catalyzed by glucose-6-phosphate dehydrogenase, *J. Am. Chem. Soc. 106*, 7263−7264.
78. Bibbs, J. A., Demuth, H. U., Huskey, W. P., Mordy, C. W., and Schowen, R. L. (1988) On the role of quantum tunneling phenomena in the catalytic power of enzymes, *J. Mol. Catal. 47*, 187−197.

79. Wolfenden, R., Snider, M., Ridgway, C., and Miller, B. (1999) The temperature dependence of enzyme rate enhancement, *J. Am. Chem. Soc. 121*, 7419−7420.
80. Doll, K. M., Bender, B. R., and Finke, R. G. (2003) The first experimental test of the hypothesis that enzymes have evolved to enhance hydrogen tunneling, *J. Am. Chem. Soc. 125*, 10877−10884.
81. Doll, K. M., and Finke, R. G. (2003) A compelling experimental test of the hypothesis that enzymes have evolved to enhance quantum mechanical tunneling in hydrogen transfer reactions: The β-eopentylcobalamin system combined with prior adocobalamin data, *Inorg. Chem. 42*, 4849−4856.
82. Padmakumar, R., Padmakumar, R., and Banerjee, R. (1997) Evidence that cobalt−carbon bond homolysis is coupled to hydrogen atom abstraction from substrate in methylmalonyl-CoA mutase, *Biochemistry 36*, 3713−3718.

BI036124G